Inorganica Chimica Acta, *191* (1992) 183–188

A fluorescent EXAFS study on the structure of the solvated cobalt(II) ion and chlorocobalt(II) complexes in hexamethylphosphoric triamide

Kazuhiko Ozutsumi*
Department of Chemistry, University of Tsukuba, Tsukuba 305 (Japan)

Kazuyuki Tohji, Yasuo Udagawa
Department of Molecular Structure, Institute for Molecular Science, Myodaiji, Okazaki 444 (Japan)

Yuriko Abe
Department of Chemistry, Faculty of Science, Nara Women's University, Nara 630 (Japan)

and Shin-ichi Ishiguro
Department of Electronic Chemistry, Tokyo Institute of Technology at Nagatsuta, Midori-ku, Yokohama 227 (Japan)

(Received July 30, 1991)

Abstract

The coordination structure of the cobalt(II) ion and its chloro complexes of low concentration (~ 20 mmol dm^{-3}) in hexamethylphosphoric triamide (HMPA) has been explored by laboratory EXAFS (extended X-ray absorption fine structure) modified for fluorescence detection. The cobalt(II) ion is four-coordinated in HMPA, unlike other oxygen-donor solvents such as water and *N,N*-dimethylformamide (DMF). The Co–O (HMPA) bond lengths within complexes are revealed to be 194(1), 195(1), 194(1) and 202(2) pm for $[Co(hmpa)_4]^{2+}$, $[CoCl(hmpa)_3]^+$, $[CoCl_2(hmpa)_2]$ and $[CoCl_3(hmpa)]^-$, respectively. The Co–O bond length is significantly shorter than that within six-coordinate $[Co(H_2O)_6]^{2+}$ (208 pm) or $[Co(dmf)_6]^{2+}$ (206 pm), and remains practically unchanged upon formation of mono- and dichloro complexes. On the other hand, the Co–Cl bond length is 224(1), 227(1) and 229(1) pm within $[CoCl(hmpa)_3]^+$, $[CoCl_2(hmpa)_2]$ and $[CoCl_3(hmpa)]^-$, respectively, all of which are appreciably shorter than that within the six-coordinate $[CoCl(H_2O)_5]^+$ (235 pm). The origin of the different thermodynamic behavior of chloro complexation of cobalt(II) in HMPA from that in DMF will be discussed on the basis of these structural data.

Introduction

The cobalt(II) ion forms a series of mononuclear $[CoCl_n]^{(2-n)+}$ ($n = 1,2,3,4$) complexes in hexamethylphosphoric triamide (HMPA) [1]. Interestingly, the complexation behavior in HMPA is remarkably different from that in *N,N*-dimethylformamide (DMF) [2]. In fact, the formation of $[CoCl]^+$ is very much enhanced in HMPA over DMF, and the complexation is evidently exothermic in the former solvent and endothermic in the latter. The result is surprising because the electron-pair donating ability of HMPA (for example, the donor number $D_N = 38.8$) is much stronger than that of DMF (26.6) [3]. Such unusual thermodynamic behavior may originate from the different coordination structure around the metal(II) ion in these solvents.

Divalent transition metal ions are usually six-coordinated in oxygen-donor solvents such as water, methanol, DMF and dimethyl sulfoxide. However, although HMPA is also an oxygen-donor solvent, these metal(II) ions cannot accommodate six HMPA molecules but only four, because HMPA is especially bulky. Indeed, various metal salts involving four HMPA molecules per metal have been prepared [4], and in the case of cobalt(II), the metal perchlorate in HMPA is blue, as it is in the solvate crystals [5–7]. Although the coordination geometries in solution have been revealed for some metal ions directly by solution X-ray diffraction and EXAFS [8–10], no detailed structural analysis of metal(II) HMPA solutions has been reported so far.

In this work we therefore aimed to determine the structure parameters of the solvated cobalt(II) ion and its chloro complexes in HMPA by EXAFS (extended X-ray absorption fine structure). Since the solubility

---

*Author to whom correspondence should be addressed.

0020-1693/92/$5.00

of the complexes in HMPA is as low as a few tens of mmol dm^{-3}, EXAFS measurements were performed by fluorescence detection of laboratory EXAFS. In a previous study [10], we reported the structure of the solvated cobalt(II) ion and the tri- and tetrachlorocobaltate(II) complexes in DMF. The structure parameters thus obtained in HMPA will be discussed in comparison with those in DMF and water.

Experimental

Materials

All chemicals used were of reagent grade. Cobalt(II) perchlorate and cobalt(II) chloride were recrystallized once from water. Cobalt(II) perchlorate HMPA solvate was prepared and dried by the same method as described elsewhere [5, 6]. Tetra-n-butylammonium chloride and lithium chloride were used without further purification, and were dried at 100 °C. Hexamethylphosphoric triamide was purified as described elsewhere [5, 6].

Six sample solutions AQ0, HMPA0, HMPA1, HMPA2, HMPA3 and AQ4 were prepared for fluorescent EXAFS measurements. The composition of the sample solutions is given in Table 1. Solutions AQ0 and AQ4 are the standard samples for EXAFS analyses. Solution AQ0 is an aqueous cobalt(II) perchlorate solution and solution AQ4 was prepared by dissolving cobalt(II) chloride in an aqueous 13 mol dm^{-3} lithium chloride solution. The two solutions contain $[Co(H_2O)_6]^{2+}$ and $[CoCl_4]^{2-}$, respectively, of known structure [8, 11]. Solution HMPA0 is a cobalt(II) perchlorate HMPA solution. Solutions HMPA1, HMPA2 and HMPA3 were prepared by dissolving copper(II) perchlorate HMPA solvate and tetra-n-butylammonium chloride in HMPA at suitable C_{Cl}/C_{Co} mole ratios. These HMPA solutions were prepared and treated under a dry nitrogen atmosphere. The mono- and dichlorocobalt(II), and trichlorocobaltate(II) complexes are the main species in the solutions, respectively.

EXAFS measurements

EXAFS spectra were measured around the cobalt K-edge on a laboratory EXAFS spectrometer [12] modified for the fluorescence detection [13] at the Institute for Molecular Science.

A rotating anode X-ray generator (Rigaku RU-200) was operated at the voltage of 12 kV and the current of 200 mA. Monochromatized X-rays were obtained by a Johansson cut bent Ge(220) crystal. Helium bags were placed along the beam path to prevent absorption by air. Sample solutions were held in a 5 mm thick glass cell with a Mylar window.

The incident X-ray intensity I_0 and the fluorescent intensity I were simultaneously measured by an ion chamber and an NaI scintillation counter of diameter two inches combined with a filter (10 μm thick iron foil), respectively. Measurements were repeated at least twice in the whole energy range. More than 1×10^6 total counts of I were obtained at each data point above the edge. An example of the observed spectra μ $(=I/I_0)$ is shown in Fig. 1.

TABLE 1. The composition of sample solutions

Solution	C_{Co} (mol dm^{-3})	C_{Cl} (mol dm^{-3})	C_{Cl}/C_{Co}
AQ0	0.0203	0	0
HMPA0	0.0210	0	0
HMPA1	0.0206	0.0206	1.00
HMPA2	0.0251	0.0505	2.01
HMPA3	0.0251	0.0895	3.57
AQ4	0.100	13	130

Analysis of EXAFS data

Background intensity other than the fluorescent intensity for the K-edge of the cobalt atom was estimated by fitting a first-order polynomial function to the pre-edge and was subtracted from the raw spectrum by extrapolation. The smooth background μ_0 was evaluated by fitting a smooth curve to the observed spectrum using an eighth-order polynomial function.

The EXAFS oscillation $\chi(k)$ was extracted and normalized as $\{\mu(k)-\mu_0(k)\}/\mu_0(k)$, where k $(=\{2m(E-E_0)\}^{1/2}/\hbar)$ is the photoelectron wave vector. The constants m and h are the mass of an electron and the planck constant, respectively, E represents the energy of the incident X-rays and E_0 is the threshold energy of a K-shell electron. The E_0 value was selected as the position of the half-height of the edge jump in

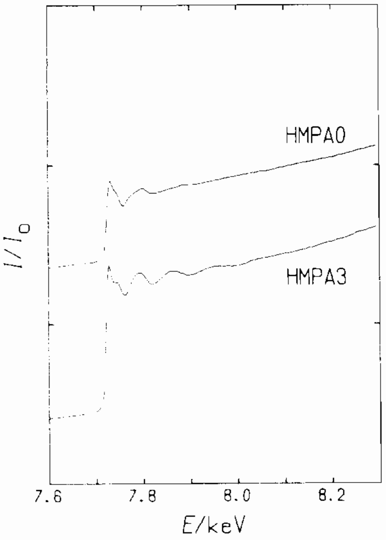

Fig. 1. Typical raw EXAFS spectra for sample solutions HMPA0 and HMPA3 by fluorescence detection.

each sample and was set to 7.722 keV throughout the analysis.

The radial structure function $F(r)$ was obtained by the Fourier transformation of the $\chi(k)$ values weighted by k^3 as

$$F(r) = (1/2\pi)^{1/2} \int_{k_{\min}}^{k_{\max}} k^3 \times \chi(k) \times W(k) \times \exp(-2ikr)\mathrm{d}k \tag{1}$$

$W(k)$ is the window function of the Hanning type [14].

The structure parameters were optimized by comparing the observed EXAFS spectra and the model function $\chi(k)_{\text{calc}}$ given by the single-electron and single-scattering theory as [15–18],

$$\chi(k)_{\text{calc}} = \Sigma\{n_j/(kr_j^2)\} \exp(-2\sigma_j^2k^2 - 2r_j/\lambda) \times F_j(\pi, k) \times \sin(2kr_j + \alpha_j(k)) \tag{2}$$

where $F_j(\pi, k)$ is the backscattering amplitudes from each of n_j scatterers j at distances r_j from the central atom. The parameter σ_j is the Debye–Waller factor and λ is the mean free path of the photoelectron. The parameter $\alpha_j(k)$ is the total scattering phase shift due to central and scattering atoms. The values of $F_j(\pi, k)$ in eqn. (2) were taken from the tables reported by Teo and Lee [19]. The phase shift $\alpha_j(k)$ was approximated by the function $a_0 + a_1k + a_2k^2 + a_3/k^3$ [20], where the a_0, a_1, a_2 and a_3 values were estimated by fitting the function to the theoretical phase shift values by Teo and Lee [19]. The theoretical values of the phase shift are given against the absolute k values and thus an improper evaluation of the E_0 value affects the interatomic distances to be determined. The E_0 value is usually treated as a parameter and estimated by the least-squares calculation applied to the structure standard. In the present analysis the a_0 and a_1 values were refined instead of the usual E_0 optimization. By comparing the Fourier filtered $k^3\chi(k)_{\text{obs}}$ values with the model function to minimize the error-square sum U $(=\Sigma k^6(\chi(k)_{\text{obs}} - \chi(k)_{\text{calc}})^2)$, the parameters a_0, a_1 and λ were first determined from the standard samples of known structure (an aqueous cobalt(II) perchlorate solution (AQ0) containing $[\text{Co(H}_2\text{O)}_6]^{2+}$ and a cobalt(II) chloride in a 13 mol dm^{-3} LiCl solution (AQ4) containing $[\text{CoCl}_4]^{2-}$ for the Co–O and Co–Cl atom pairs, respectively [8, 11]). The parameters a_0, a_1 and λ were then kept constant in the course of the structural analysis of unknown samples, while r, σ and n values were optimized as variables.

Results

The extracted EXAFS oscillations in the form of $k^3\chi(k)$ for solutions AQ0, HMPA0, HMPA1, HMPA2, HMPA3 and AQ4 (see Table 1) are shown in Fig. 2, and their Fourier transforms $|F(r)|$ in Fig. 3. It is evident from Fig. 2 that the phase of the $k^3\chi(k)$ curve of solution AQ0 is different from that of HMPA0, suggesting that these two solutions involve different local structures with respect to the cobalt(II) ion. Note that in Fig. 3 the first main peak of solution HMPA0 appears at an appreciably shorter r position compared to that of solution AQ0. Since both water and HMPA are oxygen-donor solvents, the first main peaks may be due to the Co–O (solvent) interactions. In water, the presence of the octahedral $[\text{Co(H}_2\text{O)}_6]^{2+}$ entity has been established, and its structural parameters have been deter-

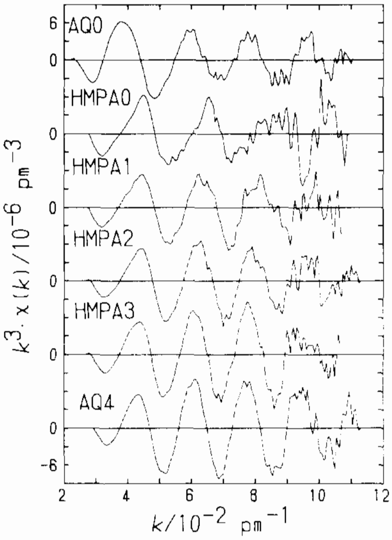

Fig. 2. The extracted EXAFS oscillations multiplied by k^3 for sample solutions. AQ0: $\text{Co(ClO}_4)_2$ in water, HMPA0: $\text{Co(ClO}_4)_2$ in HMPA, HMPA1: $[\text{CoCl}]^+$ in HMPA, HMPA2: $[\text{CoCl}_2]$ in HMPA, HMPA3: $[\text{CoCl}_3]^-$ in HMPA, AQ4: $[\text{CoCl}_4]^{2-}$ in water.

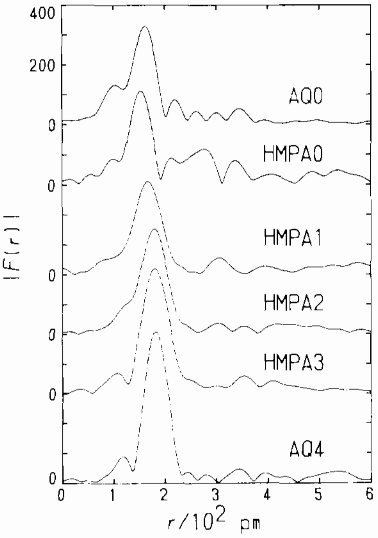

Fig. 3. The Fourier transforms $F(r)$ of the $k^3\chi(k)$ curves shown in Fig. 2, uncorrected for phase shift.

mined by X-ray diffraction [8]. In HMPA, the cobalt(II) ion exists as $[Co(hmpa)_4]^{2+}$ [1], and thus the observed peak shift toward the shorter r may be ascribed to the fact that the effective ionic radius of cobalt(II) ion is smaller under an environment of four coordination [21].

Solutions HMPA1, HMPA2 and HMPA3 involves $[CoCl]^+$, $[CoCl_2]$ and $[CoCl_3]^-$ as the predominant species, respectively [1]. All the complexes are four-coordinated according to their individual electronic spectra. In Fig. 3 the first peak position shifts gradually to the larger r, and its intensity becomes stronger with increasing the number of Co–Cl interactions within the complexes, suggesting that the first peak consists of both Co–O and Co–Cl interactions.

To obtain structure parameters for the Co–O and Co–Cl bonds, a non-linear least-squares analysis was applied to the Fourier filtered $k^3\chi(k)$ values over the range $4.5<k$ $(10^{-2}\ pm^{-1})<10.0$. The Fourier filtering was performed over the r range including the main peak in the $|F(r)|$ curve for each sample. The phase shift functions and the λ values for the Co–O and Co–Cl atom pairs were evaluated in advance from solutions AQ0 and AQ4 involving octahedral $[Co(H_2O)_6]^{2+}$ and tetrahedral $[CoCl_4]^{2-}$ of known structure, respectively [8, 11]. In the fitting procedures, bond lengths and the numbers of interactions for the Co–O and Co–Cl bonds were fixed at the literature values [8, 11], while the parameters σ, λ, a_0 and a_1 were optimized as independent variables.

The interatomic distances and Debye–Waller factors for the cobalt(II) complexes in HMPA were then refined as variables by adopting the phase functions and the λ values evaluated above. However, since the phase function and the λ value for the Co–O atom pair were estimated on the basis of octahedral $[Co(H_2O)_6]^{2+}$ in water, their transferability to the tetrahedral species must be checked. This applicability is satisfactorily established because, when the number n of the Co–O interactions was refined, together with the r and σ values, the n value converged to 3.8(1) for solution HMPA0 involving $[Co(hmpa)_4]^{2+}$. In the course of the non-linear least-squares analysis of solutions HMPA1, HMPA2 and HMPA3, since all the chloro complexes of cobalt(II) were supposed to have a four-coordination structure, the sum of the Co–O and Co–Cl interactions was fixed at four, i.e. $[CoCl(hmpa)_3]^+$, $[CoCl_2(hmpa)_2]$ and $[CoCl_3(hmpa)]^-$, and the r and σ values were refined. The r and σ values so obtained are listed in Table 2. As shown in Fig. 4, the solid curves, calculated by using the parameter values in Table 2, reproduce well the experimental points.

TABLE 2. Results of the least-squares refinements of structure parameters for cobalt(II) ion and its chloro complexes in hexamethylphosphoric triamide[a]

Complex	Interaction	r (pm)	σ (pm)	n
$[Co(H_2O)_6]^{2+}$ (in water)	Co–O	208[b, c]	7.3(2)	6[b, c]
$[Co(hmpa)_4]^{2+}$ (in HMPA)	Co–O	194(1)	5.0(1)	4[b]
$[CoCl(hmpa)_3]^+$	Co–O	195(1)	6.0(2)	3[b]
(in HMPA)	Co–Cl	224(1)	1.9(4)	1[b]
$[CoCl_2(hmpa)_2]$	Co–O	194(1)	5.3(3)	2[b]
(in HMPA)	Co–Cl	227(1)	3.5(2)	2[b]
$[CoCl_3(hmpa)]^-$	Co–O	202(2)	5.0(4)	1[b]
(in HMPA)	Co–Cl	229(1)	5.9(2)	3[b]
$[CoCl_4]^{2-}$ (in water)	Co–Cl	229[b, d]	5.4(1)	4[b, d]

Standard deviations are given in parentheses. [a] $\lambda_O = 630(20)$ and $\lambda_{Cl} = 853(38)$ pm. [b] The values were kept constant during the calculations. [c] Ref. 8. [d] Ref. 11.

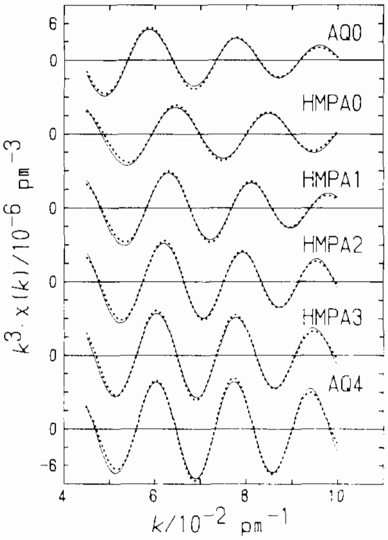

Fig. 4. The Fourier filtered $k^3\chi(k)$ curves of the main peak depicted in Fig. 3. The observed values are shown by dots and the ones calculated using parameter values in Table 2 by solid lines.

Discussion

In Table 3 the coordination bond lengths of the solvated cobalt(II) ion and its chloro complexes in HMPA, DMF and water are summarized. The Co–O bond length within $[Co(hmpa)_4]^{2+}$ is significantly shorter than that within $[Co(H_2O)_6]^{2+}$ or $[Co(dmf)_6]^{2+}$. However, the extent of bond shortening is slightly smaller than expected (16.5 pm) from the difference between effective ionic radii of cobalt(II) ion with four- and six-coordinate structure [21]. In fact, the Co–O ($OCPh_3^-$) bond length in crystals of $Co(OCPh_3)_2(thf)_2$ is 187 pm under a distorted tetrahedral environment, where $OCPh_3^-$ and THF refer to triphenylmethanolate ion and tetrahydrofuran, respectively [22]. Thus, it is supposed that bond shortening is avoided by a steric interaction between bulky HMPA molecules. The re-

TABLE 3. Coordination bond distances within the cobalt(II) ion and its chloro complexes in hexamethylphosphoric triamide, *N,N*-dimethylformamide and water

Solvent	Complex	r_{Co-O} (pm)	r_{Co-Cl} (pm)
HMPA	$[Co(hmpa)_4]^{2+}$	194(1)	
	$[CoCl(hmpa)_3]^+$	195(1)	224(1)
	$[CoCl_2(hmpa)_2]$	194(1)	227(1)
	$[CoCl_3(hmpa)]^-$	202(2)	229(1)
DMF[a]	$[Co(dmf)_6]^{2+}$	206(1)	
	$[CoCl_3(dmf)]^-$	202(1)	227(1)
	$[CoCl_4]^{2-}$		229(1)
Water[b]	$[Co(H_2O)_6]^{2+}$	208(2)	
	$[CoCl(H_2O)_5]^+$	214(1)	235(1)
	$[CoCl_4]^{2-}$		229(1)

[a] Ref. 10. [b] Refs. 8 and 11.

placement of HMPA molecules by chloride ions to form $[CoCl(hmpa)_3]^+$ or $[CoCl_2(hmpa)_2]$ may reduce steric repulsion between bulky HMPA molecules, which may lead to shortening of the Co–O (HMPA) bonds. However, the Co–O (HMPA) bond length remains practically unchanged within $[Co(hmpa)_4]^{2+}$, $[CoCl(hmpa)_3]^+$ and $[CoCl_2(hmpa)_2]$. This is not unexpected because the metal–solvent interaction is often weakened, i.e. the bond length is elongated, upon complexation of metal with chloride ions, probably due to decreasing fractional charge on the metal ion. Consequently, the bond shortening due to the reduced steric interaction may be compensated by the bond lengthening due to the decreasing fractional charge on the metal ion.

The Co–O bond length within $[CoCl_3(hmpa)]^-$, in which coordination of an HMPA molecule to the cobalt(II) ion may not be sterically hindered, is appreciably elongated compared to that within $[Co(hmpa)_4]^{2+}$. Interestingly, although the donor property of HMPA is stronger than that of DMF, both the Co–O and Co–Cl bond lengths within $[CoCl_3(hmpa)]^-$ are practically the same as those within $[CoCl_3(dmf)]^-$. Probably, the cobalt(II) ion within a trichloro complex is weak as a Lewis acid, and thus it can not distinguish solvents having different electron-pair donating abilities. This may be supported by the similar reaction enthalpy values, -8 and -6.2 kJ mol^{-1} in HMPA and DMF, respectively, for the reaction [1, 2]:

$$[CoCl_3S]^- + Cl^- \longrightarrow [CoCl_4]^{2-} + S \quad (S = \text{HMPA or DMF})$$

The Co–O bond lengths within four-coordinate complexes are all significantly smaller than those within six-coordinate complexes, indicating that the four-coordinate complexes have a stronger Co–O bond, i.e. the energy needed for breaking a Co–O bond of four coordination is larger than that of six coordination. Therefore, the fact that the formation of the monochloro complex is exothermic in HMPA but is endothermic in DMF, although the electron-pair donating ability is stronger for HMPA, may originate from a stronger Co–Cl bond within $[CoCl(hmpa)_3]^+$ than within $[CoCl(dmf)_5]^+$. In fact, the Co–Cl bond length within the $[CoCl(hmpa)_3]^+$ complex is shorter than that within $[CoCl(H_2O)_5]^+$. However, it is noted that (see Table 3) the Co–O bond length within $[CoCl(H_2O)_5]^+$ is appreciably elongated compared to that within $[Co(H_2O)_6]^{2+}$. Although the structural parameters of $[CoCl(dmf)_5]^+$ have not been obtained due to its suppressed formation in DMF, what applies for water may also apply for DMF. In contrast, the Co–O (HMPA) bond does not appreciably change upon complexation of $[CoCl(hmpa)_3]^+$. This implies that the extra energy is needed for the elongation of five Co–O bonds upon formation of $[CoCl(dmf)_5]^+$, but not upon formation of $[CoCl(hmpa)_3]^+$. Consequently, these two factors may be the major cause of the unusual thermodynamic behavior of chloro complexation of cobalt(II) in HMPA.

Acknowledgements

The present work has been financially supported, in part, by the Grant-in-Aid for Scientific Research No. 03640510 from the Ministry of Education, Science and Culture of Japan. Part of the computer calculations was carried out at the computer center of the Institute for Molecular Science in Okazaki, Japan.

References

1 Y. Abe, K. Ozutsumi and S. Ishiguro, *J. Chem. Soc., Faraday Trans. 1, 85* (1989) 3747.
2 S. Ishiguro, K. Ozutsumi and H. Ohtaki, *J. Chem. Soc., Faraday Trans. 1, 84* (1988) 2409.
3 V. Gutmann, *The Donor-Acceptor Approach to Molecular Interactions*, Plenum, New York, 1978.
4 J. T. Donoghue and R. S. Drago, *Inorg. Chem., 1* (1962) 866; *2* (1963) 1158.
5 Y. Abe and G. Wada, *Bull. Chem. Soc. Jpn., 53* (1980) 3547.
6 Y. Abe and G. Wada, *Bull. Chem. Soc. Jpn., 54* (1981) 3334.
7 W. Grzybkowski, M. Pilarczyk and L. Klinszpron, *J. Chem. Soc., Faraday Trans. 1, 84* (1988) 1551.
8 H. Ohtaki, T. Yamaguchi and M. Maeda, *Bull. Chem. Soc. Jpn., 49* (1976) 701.
9 K. Ozutsumi, S. Ishiguro and H. Ohtaki, *Bull. Chem. Soc. Jpn., 61* (1988) 945.
10 K. Ozutsumi, K. Tohji, Y. Udagawa and S. Ishiguro, *Bull. Chem. Soc. Jpn., 64* (1991) 1528.
11 H.-G. Lee, Y. Matsumoto, T. Yamaguchi and H. Ohtaki, *Bull. Chem. Soc. Jpn., 56* (1983) 443.
12 K. Tohji, Y. Udagawa, T. Kawasaki and K. Masuda, *Rev. Sci. Instrum., 54* (1983) 1482.
13 K. Tohji, T. Mizushima and Y. Udagawa, *Jpn. J. Appl. Phys., 29* (1990) 2171.

14 F. J. Harris, *Proc. IEEE, 66* (1978) 51.
15 D. E. Sayers, E. A. Stern and F. W. Lytle, *Phys. Rev. Lett., 27* (1971) 1204.
16 E. A. Stern, *Phys. Rev. B, 10* (1974) 3027.
17 E. A. Stern, D. E. Sayers and F. W. Lytle, *Phys. Rev. B, 11* (1975) 4836.
18 B. Lengeler and P. Eisenberger, *Phys. Rev. B, 21* (1980) 4507.
19 B.-K. Teo and P. A. Lee, *J. Am. Chem. Soc., 101* (1979) 2815.
20 P. A. Lee, B.-K. Teo and A. L. Simons, *J. Am. Chem. Soc., 99* (1977) 3856.
21 R. D. Shannon, *Acta Crystallogr., Sect. A, 32* (1976) 751.
22 G. A. Sigel, R. A. Bartlett, D. Decker, M. M. Olmstead and P. P. Power, *Inorg. Chem., 26* (1987) 1773.